Int. J. Electrochem. Sci., 9 **(2014)** 2491 - 2506

International Journal of
ELECTROCHEMICAL
SCIENCE
www.electrochemsci.org

Poly(lactic acid)-based Nanocomposite for Construction of Efficient Bilirubin Oxidase-Based Biocathodes and Stable Biofuel Cells

Jaroslav Filip, Rastislav Monosik, Jan Tkac[*]

Department of glycobiotechnology, Institute of chemistry, Center for glycomics, Slovak academy of sciences, Dubravska cesta 9, Bratislava 845 38, Slovak republic
[*]E-mail: jan.tkac@savba.sk

Received: 9 December 2013 / *Accepted:* 18 January 2014 / *Published:* 2 March 2014

A modification of electrode surfaces with dispersions of carbon black and consequent enzyme adsorption has been recognized as an efficient technique for construction of biofuel cells (BFCs). To achieve this, typically fluorinated polymers with a negative environmental impact are used as dispersing agents. In this work, these were replaced by an abundant, biodegradable and cost-effective biopolymer poly(lactic acid) (PLA) for construction of novel BFCs in a green and sustainable way. The electron transfer rate of bilirubin oxidase (BOD) within a biocathode, often limiting overall performance of BFCs, was greatly enhanced to the highest value of (300 ± 2) s^{-1} reported so far by introduction of a PLA matrix. The BFC was completed by a combination of a BOD biocathode with a fructose dehydrogenase bioanode, offering a power density of 57 μW cm^{-2} at 400 mV. A scanning electron microscopy of scaled up BFC device, prepared by deposition of PLA containing nanocomposites on carbon paper, revealed a highly porous structure, a feature important to deal with a limited diffusion of a biofuel and oxygen within a 3D matrix. The fructose-oxygen BFC offered an excellent operational stability comparable to the best ones reported for similar BFCs with 50% of an initial current/power observed after 10 days of storage.

Keywords: Biofuel cells, carbon black, poly(lactic acid), bioelectrocatalysis, bilirubin oxidase

1. INTRODUCTION

A general task for sustainable biotechnology is to perform chemical reactions efficiently in an economical way by taking advantages of natural catalysts – enzymes. These biocatalysts, offering high reaction rates under physiological conditions towards wide range of compounds/biofuels, have distinct advantages over inorganic catalysts, thus opening doors to „green“ and sustainable chemistry. The

"green chemistry" concept can be applied for construction of biofuel cells (BFCs), where microbial cells or isolated enzymes are employed to perform an anodic biofuel oxidation and a coupled cathodic reduction of an oxidizing agent. Thus the electricity is harnessed from a supplied substrate/biofuel in a way similar to conventional fuel cells[1-3].

The main issue regarding fabrication of BFCs is an immobilization of biocatalysts on a surface of an anode and a cathode[4]. Recently, a progress in nanotechnology allowed an effective integration of the enzymes with nanomaterials providing a high active surface area for enhanced biocatalyst´s loading, favorable redox properties, proper functional groups available for immobilization and other attractive features (reviewed for example in ref[5-7]). A substantial effort is focused on employment of carbon nanotubes (CNTs)[8-10], which can introduce high conductivity if applied in CNT/polymer or CNT/biopolymer[11] matrix composites and represent a cutting edge electrode material in a form of free-standing "bucky" CNT-based papers[12]. Moreover, CNTs can be applied for an oriented immobilization of high amount of biocatalyst molecules, what is essential for a high power output of constructed BFCs[13-16].

Another promising approach is based on a fabrication of a 3D nanoporous structures from spherical nanoparticles[17,18], which can surpass CNTs in certain applications[19], although a more detailed comparison is still lacking. For example, gold nanoparticles were reported to form a very effective and stable electrode interface without any binding polymer matrix required[18]. Carbonaceous spherical nanoparticles, much cheaper and more abundant nanomaterial compared to gold nanoparticles, can form interfacial 3D nanostructures, which were stabilized by a hydrophobic polymer matrix such as poly(vinylidene difluoride)[20,21], Teflon[22-24] or Nafion®[25, 26]. In respect to carbonaceous nanoparticles a recent study suggested that KetjenBlack has more favorable structure of pores compared to Vulcan carbon black for construction of fuel cells[27]. This is why in our previous study a KetjenBlack/chitosan-based nanocomposite was tested for construction of effective BFCs[28].

Carbon nanoparticles were tested as fillers of conductive polymer composites using synthetic polymers (polyolefine and polyamide)[29-31], biopolymers such as plasticized starch[32] or poly(lactic acid) (PLA)[33-36], employed in various applications. PLA matrix was also found to be compatible with other nanomaterials like CNTs[37, 38], graphite[39], grapheme[40, 41], silicate nanomaterials[42, 43] and metallic nanoparticles[44, 45]. Such frequent application of PLA in a preparation of diverse range of nanocomposites is not surprising because of its simple and environmentally friendly way of production[46], biodegradability[47] and also a biocompatibility of PLA matrix alone[48-51] or PLA-based nanocomposites[41,52-54]. A typical utilization of PLA-based conductive nanocomposites is for a fabrication of a diverse range of electrochemical biosensors[50,52,53,55].

In this work, PLA is for the first time employed in a construction of an enzymatic BFC based on a fructose dehydrogenase (FDH) and a bilirubin oxidase (BOD) as an anodic and a cathodic biocatalyst, respectively. The enzymes are adsorbed on an electrode surface modified with KetjenBlack/PLA dispersion and a capability of the device to be scaled-up was also studied. Operational characteristics related to electrochemical behavior of immobilized enzymes were compared with the BFC prepared from a chitosan-based nanocomposite. The study revealed that PLA

possess a more suitable environment for the BOD immobilization, thus a higher total power output can be obtained from this renewable material-based BFC compared to the chitosan-based one.

2. EXPERIMENTAL PART

2.1. Materials

Bilirubin oxidase (BOD; 8 U mg^{-1}, *Myrothecium verrucaria*), chitosan (CHI; MW = 50-190 kDa), dimethyl formamide (DMF) and single wall carbon nanotubes (CNT; d = 1.1 nm, l = 0.5–100 μm, >90% purity) were purchased from Sigma Aldrich (St. Louis, USA). Fructose dehydrogenase (FDH; 129 U mg^{-1}, *Gluconobacter oxydans*) was purchased from Sorachim (Paris, France). Carbon black "KetjenBlack EC 600-JD" (KB; Akzo Nobel Polymer Chemicals B.V., Amersfoort, Netherlands) was kindly donated by Biesterfeld Silcom s.r.o. (Prague, Czech Republic). Poly(lactic acid) (PLA) Ingeo 4060D (NatureWorks LLC, Minnetonka, USA) was kindly donated by the Polymer Institute of Slovak Academy of Sciences. Carbon paper "Toray paper" (TP) EC-TP1-090 was purchased from Electrochem, Inc. (Woburn, USA). All other reagents were of analytical grade.

2.2 Preparation of dispersions

Chitosan dispersions were prepared as described previously[28]. Briefly, KB was ground with CHI solution (0.1% in 0.3% acetic acid) in a mortar to obtain homogenous dispersion, which was consequently mixed with CNT/CHI dispersion (5 mg ml^{-1}, obtained by 30 min sonication of CNT in CHI). Concentrations of KB and CHI in the final KB/CNT-CHI nanocomposite were 0.67 mg ml^{-1} and 4.3 mg ml^{-1}, respectively. Similarly, KB dispersion in PLA was prepared by grinding KB in a mortar together with PLA solution (0.1% in DMF).

2.3 Preparation of (bio)electrodes

Glassy carbon electrodes (GCE; geometric surface area of 0.071 cm^2; Bioanalytical systems, USA) were polished using aluminium slurry (0.3 μm, Buehler, USA), rinsed with deionised water (DW) and sonicated for 30 s in DW. On a surface of clean electrode the desired amount of prepared dispersion was pipetted and left to dry out at ambient air. Thus, prepared electrodes were denoted to as GCE|KB/CNT-CHI and GCE|KB-PLA. For construction of high surface area electrodes, strips of TP (approx. 5 x 30 mm) were dipped in the KB-PLA dispersion for 10 s with consequent drying out and the electrodes obtained are labelled as TP|KB-PLA. For preparation of chitosan-based high surface area electrodes, the same strips of TP were made more hydrophilic by soaking them in ethanol for 10 min. Consequent soaking of TP in CNT/KB-CHI dispersion was performed for 1 h with subsequent drying out and resulted electrodes are labelled as TP|CNT/KB-CHI.

Prepared GCE|KB-PLA, TP|KB-PLA and TP|CNT/KB-CHI electrodes were incubated with solutions of FDH (3 U μl^{-1}; 0.1 M acetate buffer, pH 5) or BOD (0.025 U μl^{-1}; 0.1 M acetate buffer, pH

6) using amounts indicated in the text. Prepared bioelectrodes are denoted to as GCE|KB-PLA|FDH(BOD), TP|KB-PLA|FDH(BOD) and TP|CNT/KB-CHI|FDH(BOD) and were either tested or stored in 0.1 M acetate buffer (pH 5 and 6 for FDH and BOD-based electrodes, respectively).

2.4 Instrumental methods

All electrodes were separately tested using cyclic voltammetry (CV), BFC characterization was performed using chronopotentiometry and chronoamperometry. For electrochemical experiments a potentiostat/galvanostat PGSTAT 128N (Ecochemie, Utrecht, Netherlands) was used. Measurements were done in an electrochemical cell filled with a buffer, which was aerated using air bubbling or deaerated using N_2 bubbling. A three electrode system was used with modified GCE or TP electrodes as working and Pt disc and Ag|AgCl|3 M KCl as auxiliary and referent electrodes, respectively.

TP|KB-PLA and TP|KB/CNT-CHI dispersions were also characterized using scanning electron microscope JSM-7600F (JEOL, Tokyo, Japan).

3. RESULTS AND DISCUSSION

3.1 Bioelectrodes and biofuel cells prepared on GCE

The first step in the construction of BFCs was to check the ability of KB to form a stable dispersion in a PLA solution. For this purpose, our previously reported protocols were adapted[28], i.e. KB was mixed with PLA (0.1% in dimethylformamide) and ground in a mortar. A dispersion obtained with an initial KB concentration of 13 mg ml^{-1} did not form a mechanically stable film on the electrode surface, most likely because of high KB content. Thus, dispersions with KB concentration of 4.3 mg ml^{-1}, which exhibited good stability after drying out, were applied in the following experiments. Cyclic voltammetry of GCE|KB-PLA electrodes revealed high capacitance currents on electrodes modified by the dispersion with a low KB concentration, indicating that in this case high amount of KB nanoparticles are interconnected and retained on the electrode surface providing a high electroactive surface area (Fig. 1A).

GCE|KB-PLA electrodes were further tested for their enzyme-adsorption capability by an overnight incubation with FDH and BOD solutions. Firstly, an influence of a PLA concentration (0.1, 1.0 and 2.0%) on a final biocatalytic current was assessed by cyclic voltammetry, revealing that 0.1% concentration of PLA is the best for preparation of both for the bioanode and the biocathode (Fig. S1). It can be concluded that, upon an application of the PLA-enriched dispersions, individual KB nanoparticles become rather isolated by an abundant biopolymer, thus an electron transfer through an extra PLA coating is substantially restricted. The optimized bioanode GCE|KB-PLA|FDH exhibited a current density of (479 ± 80) μA cm^{-2} and the biocathode GCE|KB-PLA|BOD a current density of (255 ± 42) μA cm^{-2} (Fig. 1B), both working without a need for addition of any redox shuttles, what is a mode of operation not requiring a separation of the bioanode from the biocathode by a membrane.

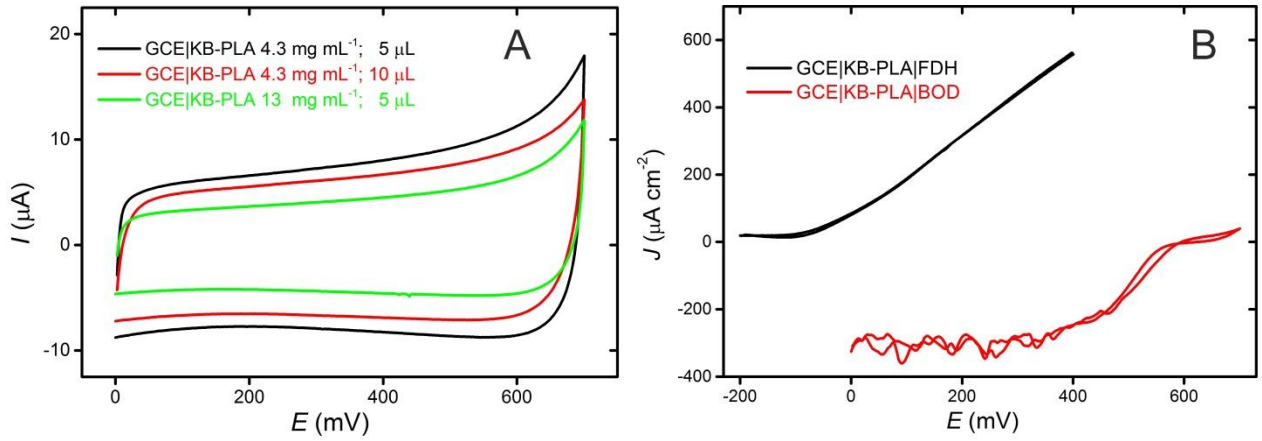

Figure 1. A – Cyclic voltammograms of GCE modified by 5 µl of KB-PLA (4.3 mg ml^{-1} of KB – black line; 13 mg ml^{-1} of KB – green line) and 10 µl of KB-PLA (4.3 mg ml^{-1} of KB – red line). All measurements were done in 0.1 M acetate buffer at pH 6.0. **B** – Background corrected voltammograms of the optimized GCE|KB/PLA|FDH bioanode (black line, run from -200 to 400 mV in a 0.1 M acetate buffer pH 5.0 containing 0.2 M fructose) and the GCE|KB/PLA|BOD biocathode (red line, run from 700 to 0 mV in an aerated 0.1 M acetate buffer pH 6). All measurements were done at a scan rate of 50 mV s^{-1}.

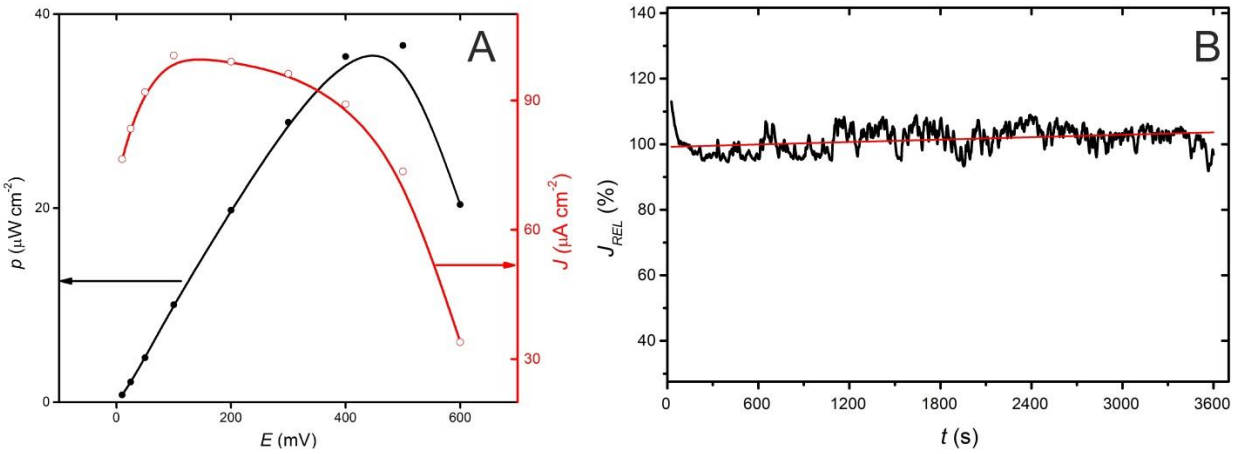

Figure 2. A – A power (left Y axis, black full dots and line) and a current (right Y axis, red empty dots and line) density as a function of a potential applied between the bioanode and the biocathode for the GCE|KB/PLA|enzyme BFC. **B** – Stability of a current density for the BFC biased at 300 mV measured after the current response was left to stabilize for 2 min. All measurements were performed in an aerated 0.1 M acetate buffer containing 0.2 M fructose at pH 6.0.

A stability of a current density output for the biocathode was tested with no decrease observed within 2.2 h, while a current density of the bioanode decreased to 55% of the initial value within the same timeframe (Fig. S2). This is the result of a low intrinsic stability of FDH, being a membrane protein composed of 3 subunits[56], rather than a mechanical instability of the interfacial layer. Finally, the optimized bioanode and the biocathode were assembled together into the fructose-oxygen

BFC with a maximum power density of 57 μW cm^{-2} at 400 mV and with an open circuit potential (OCP) of 680 mV. The performance of the BFC is shown in Fig. 2A.

The BFC device exhibited an excellent operational stability detected as an output current density at a potential of 300 mV applied between the bioanode and the biocathode (Fig. 2B). Such stability of the BFC performance is comparable or better than for previously published fructose-oxygen BFCs[14,18,20].

3.2 Bioelectrodes and biofuel cells prepared on TP

After the optimization of KB-PLA dispersion composition, a scale-up of the device was tested by applying the KB-PLA dispersion on a surface of carbon paper (TP) strips. This substrate provides a high geometric surface area of prepared electrodes plus there is also an intrinsic microstructure in an addition to a geometrical surface. It was visually checked that, even after a short (10 s) dipping of TP into the KB-PLA dispersion, nanoparticles formed a stable coating on the surface of the TP electrode. A good compatibility of the TP substrate and KB-PLA dispersion was additionally confirmed by SEM. It can be seen that KB particles dispersed in PLA are attached on a surface of TP fibers (Fig. 3A and 3C) while a chitosan-based composite tends to form a homogenous surface film without a penetration inside the TP microstructure (Fig. 3B). A highly porous structure within KB-PLA nanocomposite deposited on TP (Fig. 3C), is a feature important to deal with a limited diffusion of a biofuel and oxygen within a 3D matrix.

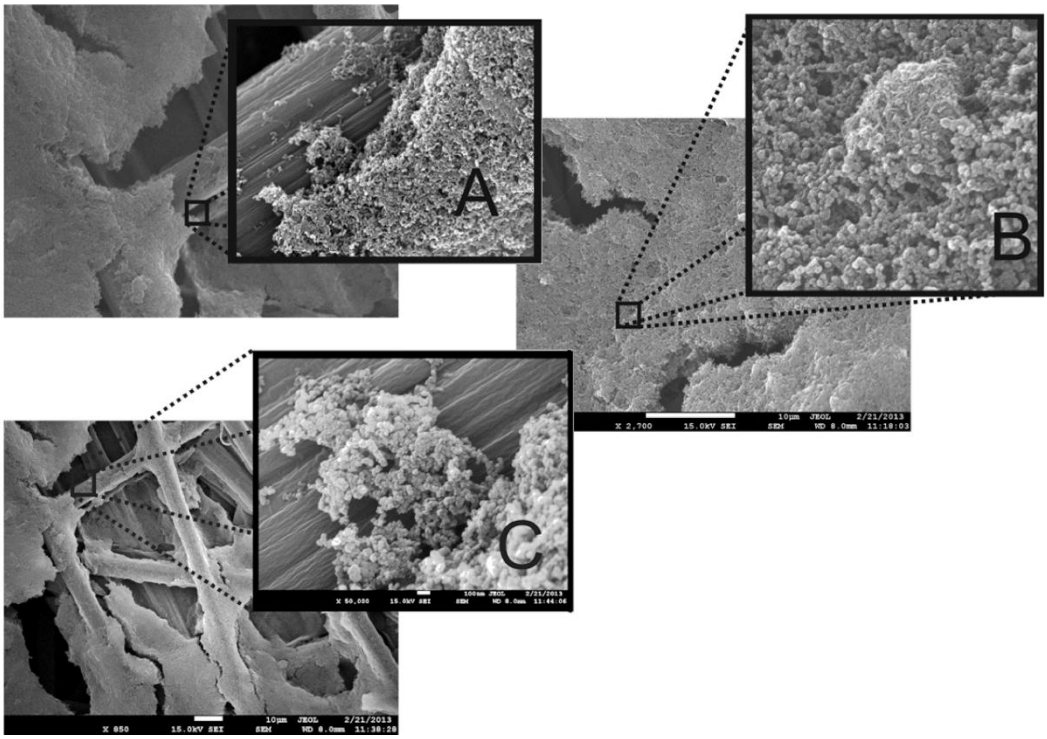

Figure 3. SEM images of the optimized TP|KB/PLA (**A**; magnification 2,040x and 30,000x), the TP|KB-CNT/CHI **(B**; magnification 2,700x and 30,000x) and the TP|KB/PLA electrodes (**C**; magnification 8,500x and 50,000x).

After incubation of the TP|KB-PLA electrodes with FDH (48 U) and BOD (0.88 U) solution in the same way as for modification of GCE electrodes, the electrodes exhibited maximum anodic and cathodic current densities of (405 ± 50) and (219 ± 34) μA cm^{-2} (Fig. S3), respectively. These values are only slightly lower compared to modified GCE electrodes. Interestingly, when the BFC was constructed from the biocathode TP|KB-PLA|BOD and the bioanode TP|KB-PLA|FDH, a maximum power density of 33 μW cm^{-2} at 300 mV and an OCP of 600 mV were found. Thus, not only the power density of TP-based BFC is lower compared to the BFC based on GCE (33 vs. 57 μW cm^{-2}), but OCP (600 vs. 680 mV), as well, due to intrinsic losses[57].

A storage stability of the TP-based BFC was tested for 13 days by a 3 h continuous reading of an amperometric response of the device in particular days at 300 mV applied between the bioanode and the biocathode. Between the measurements, the electrodes were stored in 0.1 M acetate buffer pH 5.0 (bioanode) or in 0.1 M acetate buffer pH 6.0 (biocathode) at 4°C. The study showed that, after 2 days of storage, the detected current output did not decrease and after 10 days of storage, i.e. total 22 h of current production, 39% drop in current output was detected (Fig. S4). This is similar to 37% decrease of an initial power output after 12 h of a continuous operation of KB/PVDF-based fructose-O_2 BFC reported by Kamitaka[20]. 15% drop during 12 hours of operation was reported by Murata et al., who studied BOD and FDH adsorbed on bare and mercaptoethanol-modified gold nanoparticles, respectively[18]. The same drop, but after 24 hours of operation, was achieved with a BFC based on oxidized carbon nanotubes[14] what points out the advantage of a chemisorption in contrast to a simple physisorption and may represent an efficient way for further stability increase of our PLA-based device. Nevertheless, it can be concluded that PLA is perfectly equal to PVDF from the point of view of stability of adsorbed FDH and BOD.

The features of TP|KB-PLA-based BFCs were compared to a device based on dispersion of KB (4.3 mg ml^{-1}) and CNT (0.67 mg ml^{-1}) in chitosan, described in our previous study[28]. CV of the constructed TP|KB/CNT-CHI|FDH bioanode and TP|KB/CNT-CHI|BOD biocathode were first investigated separately under the same conditions as in the case of PLA-based bioelectrodes. Average biocatalytic current densities of (410 ± 29) and (83 ± 19) μA cm^{-2} were revealed at the bioanode and the biocathode, respectively, and the BFC assembled from these bioelectrodes showed only a maximum power density of 12 μW cm^{-2} at 300 mV with an OCP of only 450 mV (data not shown).

3.3 Insights into heterogeneous enzymatic catalysis on the bioanodes and the biocathodes

The aforementioned experiments have proved that KB/PLA nanocomposite can be used for a simple and economical construction of mediator-less one compartment fructose-oxygen BFCs. The maximum power output obtained was similar to a previously reported device based on KB and CNT dispersed in chitosan[28]. However, PLA-based BFC possessed a higher OCP value (680 vs. 655 mV) and a maximum power density was detected at a higher potential (400 vs. 300 mV) compared to CHI-based BFC, suggesting a better proton conductivity of PLA-based nanocomposite compared to a chitosan-based one.

Both anodic and cathodic biocatalytic curves were fitted according to Ikeda[58] with more details given in the supplementary information file together with some examples about fitting

reliability (Fig. S5). Calculated heterogeneous electron transfer (ET) rate constant k^0 and an active enzyme surface coverage for each type of electrode are summarized in Table 1. An electrocatalytic activity of FDH (Fig. S6) and its surface coverage was only slightly lower on the CHI-based interface compared to the PLA nanocomposite (Table 1) proving that PLA-based matrix is a bit more favorable for preparation of fructose BFCs with integration of FDH as an anodic catalyst compared to CHI nanocomposite. An electrocatalytic activity of BOD dramatically changed (Fig. S7) on various nanocomposites with k^0 reaching the highest value of (300 ± 2) s^{-1} on the biocathode GCE|KB-PLA|BOD and the lowest value of (32 ± 4) s^{-1} on the biocathode TP|KB/CNT-CHI|BOD (Table 1). Calculated k^0 value of (300 ± 2) s^{-1} is very similar to the highest electron transfer rate of BOD observed in a solution (250-400 s^{-1})[59-61] and much higher than previously observed heterogeneous electron transfer rates of BOD of (1-130 s^{-1})[62], (45-170 s^{-1})[59], 59 s^{-1}(ref[63]), (70-140 s^{-1})[64], 74 s^{-1}(ref[60]) and (80-100 s^{-1})[65] obtained at different pH on various modified electrodes. Thus, it is obvious that PLA strongly supports adsorption of BOD in such a way that significantly enhanced electron exchange between BOD and nanoparticles is possible. A significantly lower k^0 = (113 ± 6) s^{-1} for BOD adsorbed on PLA nanocomposite deposited on TP (TP|KB-PLA|BOD) compared to k^0 = (300 ± 2) s^{-1} for BOD adsorbed on PLA nanocomposite deposited on GCE (GCE|KB-PLA|BOD) is most likely due to adsorption of fraction of BOD molecules directly on TP fibers (TP|BOD) in a way not efficient for bioelectroreduction of oxygen with k^0 = (52 ± 4) s^{-1} (Table 1).

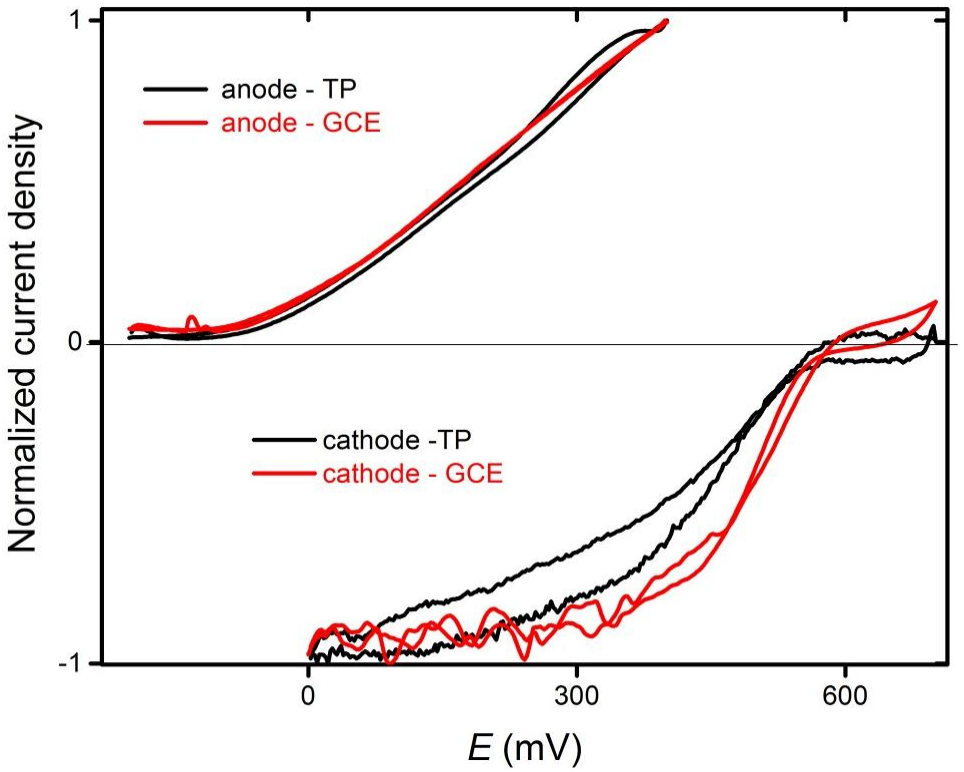

Figure 4. Normalized biocatalytical background-corrected currents obtained on TP|KB-PLA|enzymes and GCA|KB-PLA|enzymes bioanodes and biocathodes, respectively. Solid lines represent CVs on TP|KB-PLA and dashed line on GCE|KB-PLA bioanodes and biocathodes. Measurements were done in a 0.1 M acetate buffer at pH 6.0 (biocathodes) or at pH 5.0 (bioanodes).

A much lower kinetics of oxygen reduction with BOD adsorbed on the TP|KB-PLA compared to the GCE|KB-PLA can be directly seen in Fig. 4 showing normalized bioelectrocatalytic waves. A dramatic change in the surface coverage of BOD on various biocathodes spanning the range from (2.1 ± 0.2) to (10.5 ± 1.9) pmol cm^{-2} was observed, as well (Table 1). These results indicate that PLA nanocomposite not only promotes high electron transfer rate, but allows adsorbing more BOD molecules within a 3D matrix deposited on TP (i.e. $\Gamma = (9.3 \pm 0.6)$ pmol cm^{-2} for TP|KB-PLA|BOD compared to $\Gamma = (4.3 \pm 0.8)$ pmol cm^{-2} for TP|KB/CNT-CHI|BOD) (Table 1).

Table 1. Calculated heterogeneous electron transfer rate constants k^0 (s^{-1}) and an enzyme surface coverage Γ (pmol cm^{-2}) for particular bioanodes and biocathodes

Bioelectrode configuration	k^0 (s^{-1})	Γ (pmol cm^{-2})
GCE|KB-PLA|FDH	14.6 ± 0.7	22.0 ± 3.3
GCE|KB/CNT-CHI|FDH	10.3 ± 0.3	15.7 ± 3.7
TP|KB-PLA|FDH	11.0 ± 1.0	19.4 ± 2.6
TP|KB/CNT-CHI|FDH	9.7 ± 2.6	18.1 ± 1.2
GCE|KB-PLA|BOD	300 ± 2	10.5 ± 1.9
GCE|KB/CNT-CHI|BOD	46 ± 24	9.4 ± 2.2
TP|KB-PLA|BOD	113 ± 6	9.3 ± 0.6
TP|KB/CNT-CHI|BOD	32 ± 4	4.3 ± 0.8
TP|BOD	52 ± 4	2.1 ± 0.2

4. CONCLUSIONS

To the best of our knowledge, this study is the first one showing application of the KB-PLA nanocomposite for construction of a BFC. Even though a maximum power output of the PLA-based BFC of 57 μW cm^{-2} cannot compete with much higher power densities reported in previous studies[13-15, 18, 20, 21], the power output observed is in the "middle zone" of the power outputs of the BFC devices based on glucose oxidase (52 μW cm^{-2})[21], glucose dehydrogenase (39 μW cm^{-2})[19], alcohol dehydrogenase (48 μW cm^{-2})[66], just to name few of them. Our study is a solid foundation for further development of the high performance KB-PLA-based BFC. The most attractive features of such a concept are utilization of environmentally-friendly and cost-effective binding matrix of PLA for making conductive nanocomposites. Moreover, the best interfacial coupling of BOD with electrodes in terms of efficiency of electron transfer rate with $k^0 = (300 \pm 2)$ s^{-1} (Table 1) observed to date together with ability to deposit KB-PLA matrix along TP fibers (Fig. 3C), with excellent stability of the biocathodes and high storage stability of the BFC are "must have" components for increasing overall power output of such devices for example by using a very promising material - reticulated vitreous carbon[67]. Moreover, there is still a space for power output enhancement by adjusting a BFC configuration, for example by using so called air breathing cathodes, which eliminates a slow oxygen diffusion rate in aqueous solutions.

ACKNOWLEDGEMENTS
The financial support from SAV-FM-EHP-2008-04-04, from the Slovak research and development agency APVV 0282-11 and from VEGA 1/0229/12 is acknowledged. Authors would like to thank Dr. Martin Nosko for making SEM images.

References

1. L. B. Wingard Jr, C. H. Shaw, J. F. Castner, *Enzyme Microb. Tech.* 4 (1982) 137.
2. D. Leech, P. Kavanagh, W. Schuhmann, *Electrochim Acta* 84 (2012) 223.
3. B. E. Logan, *Microbial Fuel Cells*. Wiley, (2008)
4. W. J. Chen, M. H. Lee, J. L. Thomas, P. H. Lu, M. H. Li, H. Y. Lin, *ACS Appl. Mater. Interfaces* 5 (2013) 11123.
5. T. Tamaki, *Top. Catal.* 55 (2012) 1162.
6. S. D. Minteer, *Top. Catal.* 55 (2012) 1157.
7. C. Pan, J. LuoJ. Zhu, *Nano. Res.* 4 (2011) 1099.
8. G.-E. Anthony, L. Chenghong, H. B. Ray, *Nanotechnology* 13 (2002) 559.
9. M. B. Fischback, et al., *Electroanalysis* 18 (2006) 2016.
10. L. Zhang, M. Zhou, D. Wen, L. Bai, B. Lou, S. Dong, *Biosens. Bioelectron.* 35 (2012) 155.
11. X. Zhao, X. Lu, W. T. Y. Tze, J. Kim, P. Wang, *ACS Appl. Mater. Interfaces* 5 (2013) 8853.
12. C. W. Narváez Villarrubia, R. A. Rincón, V. K. Radhakrishnan, V. Davis, P. Atanassov, *ACS Appl. Mater. Interfaces* 3 (2011) 2402.
13. J. Kim, K. H. Yoo, *Phys. Chem. Chem. Phys.* 15 (2013) 3510.
14. T. Miyake, K. Haneda, S. Yoshino, M. Nishizawa, *Biosens. Bioelectron.* 40 (2013) 45.
15. T. Miyake, S. Yoshino, T. Yamada, K. Hata, M. Nishizawa, *J. Am. Chem. Soc.* 133 (2011) 5129.
16. S. Yoshino, T. Miyake, T. Yamada, K. Hata, M. Nishizawa, *Adv. Energy Mater.* 3 (2013) 60.
17. S. Lee, B. S. Ringstrand, D. A. Stone, M. A. Firestone, *ACS Appl. Mater. Interfaces* 4 (2012) 2311.
18. K. Murata, K. Kajiya, N. Nakamura, H. Ohno, *Energy Environ. Sci.* 2 (2009) 1280.
19. M. Zhou, L. Deng, D. Wen, L. Shang, L. Jin, S. Dong, *Biosen. Bioelectron.* 24 (2009) 2904.
20. Y. Kamitaka, S. Tsujimura, N. Setoyama, T. Kajino, K. Kano, *Phys. Chem. Chem. Phys.* 9 (2007) 1793.
21. T. Miyake, M. Oike, S. Yoshino, Y. Yatagawa, K. Haneda, H. Kaji, M. Nishizawa, *Chem. Phys. Lett.* 480 (2009) 123.
22. R. Kontani, S. Tsujimura, K. Kano, *Bioelectrochemistry* 76 (2009) 10.
23. G. P. M. K. Ciniciato, C. Lau, A. Cochrane, S. S. Sibbett, E. R. Gonzalez, P. Atanassov, *Electrochim. Acta* 82 (2012) 208.
24. I. Asano, Y. Hamano, S. Tsujimura, O. Shirai, K. Kano, *Electrochemistry* 80 (2012) 324.
25. A. Habrioux, K. Servat, S. Tingry, K. B. Kokoh, *Electrochem. Commun.* 11 (2009) 111.
26. A. Habrioux, T. Napporn, K. Servat, S. Tingry, K. B. Kokoh, *Electrochim. Acta* 55 (2010) 7701.
27. T. Soboleva, K. Malek, Z. Xie, T. Navessin, S. Holdcroft, *ACS Appl. Mater. Interfaces* 3 (2011) 1827.
28. J. Filip, J. Šefčovičová, P. Gemeiner, J. Tkac, *Electrochim. Acta* 87 (2013) 366.
29. J. Yu, L. Q. Zhang, M. Rogunova, J. Summers, A. Hiltner, E. Baer, *J. Appl. Polym. Sci.* 98 (2005) 1799.
30. A. Fathi, K. Hatami, B. P. Grady, *Polym. Eng. Sci.* 52 (2012) 549.
31. R. Socher, B. Krause, S. Hermasch, R. Wursche, P. Pötschke, *Compos. Sci. Technol.*71 (2011) 1053.
32. X. Ma, P. R. Chang, J. Yu, P. Lu, *Carbohyd. Polym.* 74 (2008) 895.
33. H. Tsuji, Y. Kawashima, H. Takikawa, S. Tanaka, *Polymer* 48 (2007) 4213.
34. N. Wang, X. Zhang, X. Ma, J. Fang, *Polym. Degrad. Stabil.* 93 (2008) 1044.
35. Q. Zhijun, Z. Xingxiang, W. Ning, F. Jianming, *Polym. Composite.* 30 (2009) 1576.

36. Z. Su, Q. Li, Y. Liu, W. Guo, C. Wu, *Polym. Eng. Sci.* 50 (2010) 1658.
37. J. E. Oliveira, V. Zucolotto, L. H. Mattoso, E. S. Medeiros, *J. Nanosci. Nanotechnol.* 12 (2012) 2733.
38. P. G. Seligra, F. Nuevo, M. Lamanna, L. Famá, *Compos. Part B-Eng.* 46 (2013) 61.
39. M. Murariu, et al., *Polym. Degrad. Stabil.* 95 (2010) 889.
40. Y. Shen, T. Jing, W. Ren, J. Zhang, Z.-G. Jiang, Z.-Z. Yu, A. Dasari, *Compos. Sci. Technol.* 72 (2012) 1430.
41. A. M. Pinto, S. Moreira, I. C. Gonçalves, F. M. Gama, A. M. Mendes, F. D. Magalhães, *Colloid. Surface. B* 104 (2013) 229.
42. S. Solarski, M. Ferreira, E. Devaux, *Polym. Degrad. Stabil.* 93 (2008) 707.
43. K. Prakalathan, S. Mohanty, S. K. Nayak, *J. Reinf. Plast. Compos.* 31 (2012) 1300.
44. Y. Li, C. Chen, J. Li, X. S. Sun, *Polymer* 52 (2011) 2367.
45. Y. H. Li, X. S. Sun, *J. Biobased Mater. Bio.* 5 (2011) 452.
46. H. R. Kricheldorf, *Chemosphere* 43 (2001) 49.
47. J. M. Anderson, M. S. Shive, *Adv. Drug Deliv. Rev.* 28 (1997) 5.
48. C. C. Lin, C. C. Co, C. C. Ho, *Biomaterials* 26 (2005) 3655.
49. D. Li, M. W. Frey, D. Vynias, A. J. Baeumner, *Polymer* 48 (2007) 6340.
50. W. Zheng, J. Li, Y. F. Zheng, *J. Electroanal. Chem.* 621 (2008) 69.
51. J. E. Oliveira, E. S. Medeiros, L. Cardozo, F. Voll, E. H. Madureira, L. H. C. Mattoso, O. B. G. Assis, *Mater. Sci. Eng. C Mater. Biol. Appl.* 33 (2013) 844.
52. Q. Wei, T. Li, G. Wang, H. Li, Z. Qian, M. Yang, *Biomaterials* 31 (2010) 7332.
53. X. Wu, H. Jiang, J. Zheng, X. Wang, Z. Gu, C. Chen, *J. Electroanal. Chem.* 656 (2011) 174.
54. M. Persson, G. S. Lorite, S.-W. Cho, J. Tuukkanen, M. Skrifvars, *ACS Appl. Mater. Interfaces* 5 (2013) 6864.
55. D. Li, M. W. Frey, A. J. Baeumner, *J. Membr. Sci.* 279 (2006) 354.
56. J. Tkac, J. Svitel, I. Vostiar, M. Navratil, P. Gemeiner, *Bioelectrochemistry* 76 (2009) 53.
57. X. Wu, F. Zhao, J. R. Varcoe, A. E. Thumser, C. Avignone-Rossa, R. C. T. Slade, *Biosens. Bioelectron.* 25 (2009) 326.
58. T. Ikeda, D. Kobayashi, F. Matsushita, T. Sagara, K. Niki, *J. Electroanal. Chem.* 361 (1993) 221.
59. S. Tsujimura, T. Nakagawa, K. Kano, T. Ikeda, *Electrochemistry* 72 (2004) 437.
60. P. Ramirez, N. Mano, R. Andreu, T. Ruzgas, A. Heller, L. Gorton, S. Shleev, *Biochim. Biophys. Acta* 1777 (2008) 1364.
61. A. Shimizu, et al., *J. Biochem.*125 (1999) 662.
62. K. Otsuka, T. Sugihara, Y. Tsujino, T. Osakai, E. Tamiya, *Anal. Biochem.* 370 (2007) 98.
63. J. Lim, N. Cirigliano, J. Wang, B. Dunn, *Phys. Chem. Chem. Phys.* 9 (2007) 1809.
64. M. Tominaga, M. Otani, M. Kishikawa, I. Taniguchi, *Chem. Lett.* 35 (2006) 1174.
65. K. Schubert, G. Goebel, F. Lisdat, *Electrochim. Acta* 54 (2009) 3033.
66. Y. M. Yan, O. Yehezkeli, I. Willner, *Chem. Eur. J.* 13 (2007) 10168.
67. V. Flexer, J. Chen, B. C. Donose, P. Sherrell, G. G. Wallace, J. Keller, *Energy Environ. Sci.* 6 (2013) 1291.

SUPPLEMENTARY INFORMATION:

Nonlinear fitting

$$j = \frac{nF\Gamma k_C}{1 + \frac{k_C}{k_f} + \frac{k_b}{k_f}} \quad (1)$$

$$k_f = k^0 \exp\left[(1-\alpha)\left(\frac{nF}{RT}\right)\left(E - E^{0'}\right)\right] \quad (2)$$

$$k_b = k^0 \exp\left[-\alpha\left(\frac{nF}{RT}\right)\left(E - E^{0'}\right)\right] \quad (3)$$

n – number of exchanged electrons (1 for heterogeneous ET); F – Faraday constant; Γ – an active enzyme surface concentrantion; k_C – intramolecular ET rate; k_f and k_b – forward and backward rate constants for an electron exchange between enzyme and electrode; k^0 – heterogeneous ET rate constant; α – transfer coeficcient; $E^{0'}$ – redox potential of the active site directly involved in exchange of electrones with electrode; R – molar gas constant; T – temperature.

Both anodic and cathodic bioelectrocatalyses were assumed to be fitted by a model described by equations 1 – 3 (ref[s1, s2]), where an electron exchange rate between an enzymatic active site (heme c in FDH and pressumably a T1 active site in BOD) and an electrode interface is represented by a parameter k^0. This parameter, together with Γ and α were treated as dependent calculated parametres. $E^{0'}$ a was determined to be – 85 mV for FDH and 510 mV for BOD, based on our previous experiments. Intramolecular ET rate k_C = 250 s^{-1} was used for both enzymes according to values in literature[s1, s3].

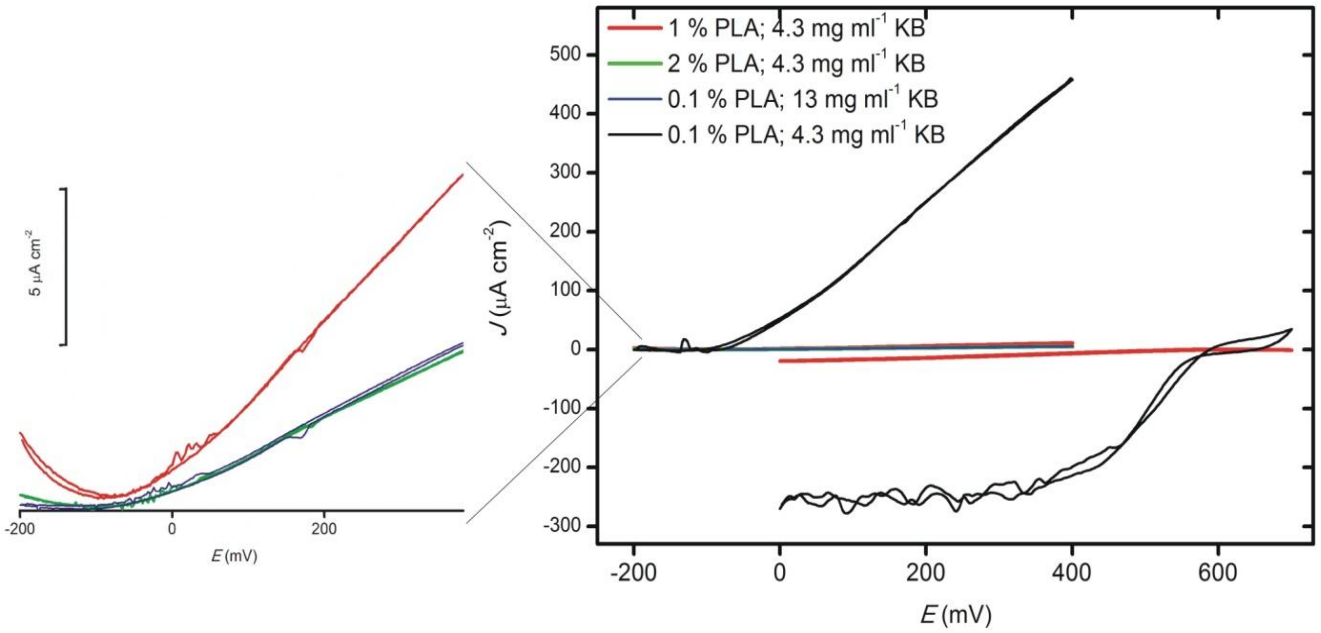

Figure S1. CVs of GCE|KB/PLA|FDH anodes and GCE|KB/PLA|BOD cathodes prepared from GCE modified with 1% (red), 2% (green) and 0.1% (black) PLA containing 4.3 mg ml^{-1} KB and with 0.1% PLA containing 13 mg ml^{-1} KB (blue). All measurements were done in 0.1 M aerated acetate buffer at pH 6.0 for the biocathodes or in 0.1 M deaerated acetate buffer containing 0.2 M fructose at pH 5.0 for the bioanodes. CVs were acquired by running measurements at a scan rate of 50 mV s^{-1}.

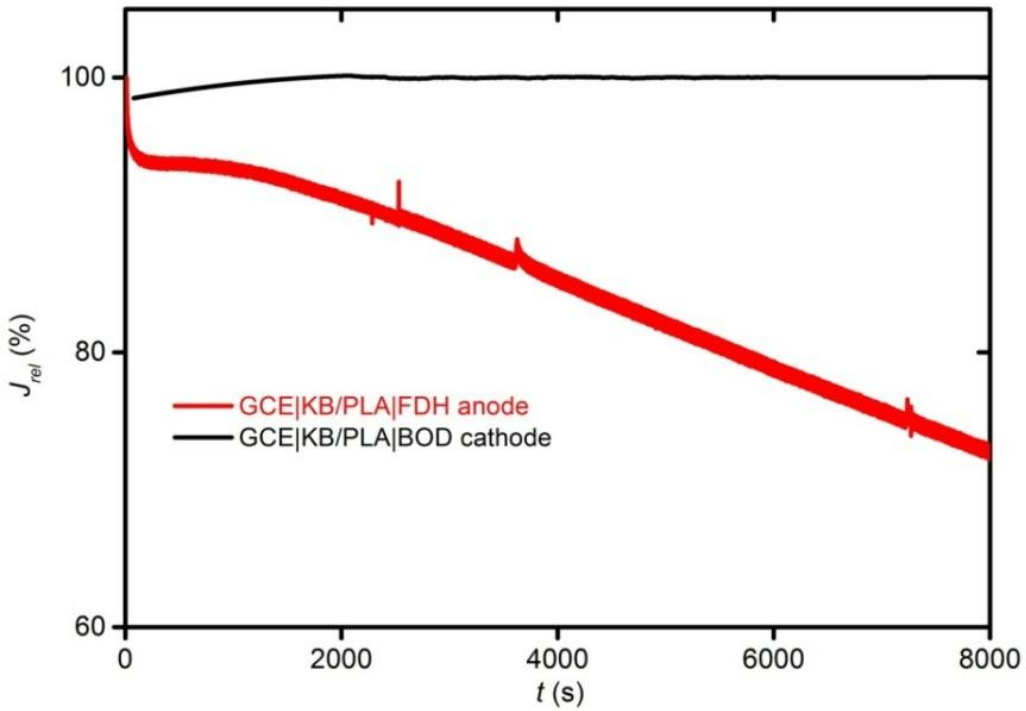

Figure S2. Chronoamperometric response observed on the GCE|KB/PLA|FDH bioanode and on the GCE|KB/PLA|BOD biocathode. Measurements were done in 0.1 M aerated acetate buffer pH 6.0 at a potential of 0 mV (the biocathode) or 0.1 M deaerated acetate buffer containing 0.2 M fructose at pH 5.0 at a potential of 350 mV (the bioanode).

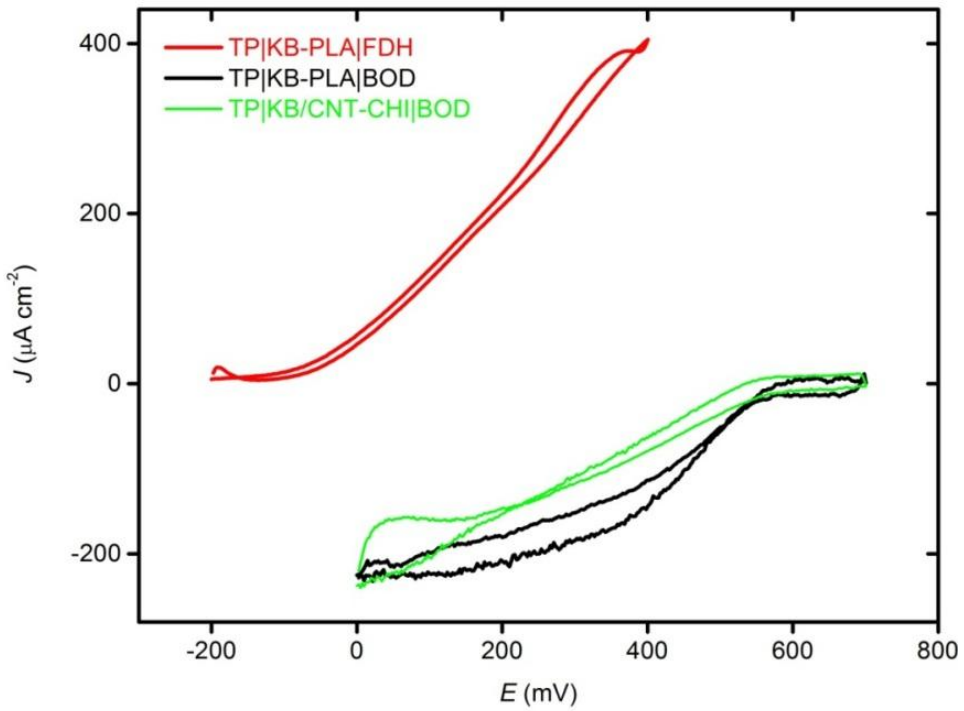

Figure S3. CVs of the TP|KB-PLA|FDH bioanode (red curve), the TP|KB-PLA|BOD (black curve) and the TP|KB/CNT-CHI|BOD (green curve) biocathodes. Measured in 0.1 M aerated acetate buffer at pH 6.0 (biocathodes) or in 0.1 M deaerated acetate buffer containing 0.2 M fructose at pH 5.0 (the bioanode) at a scan rate of 50 mVs^{-1}.

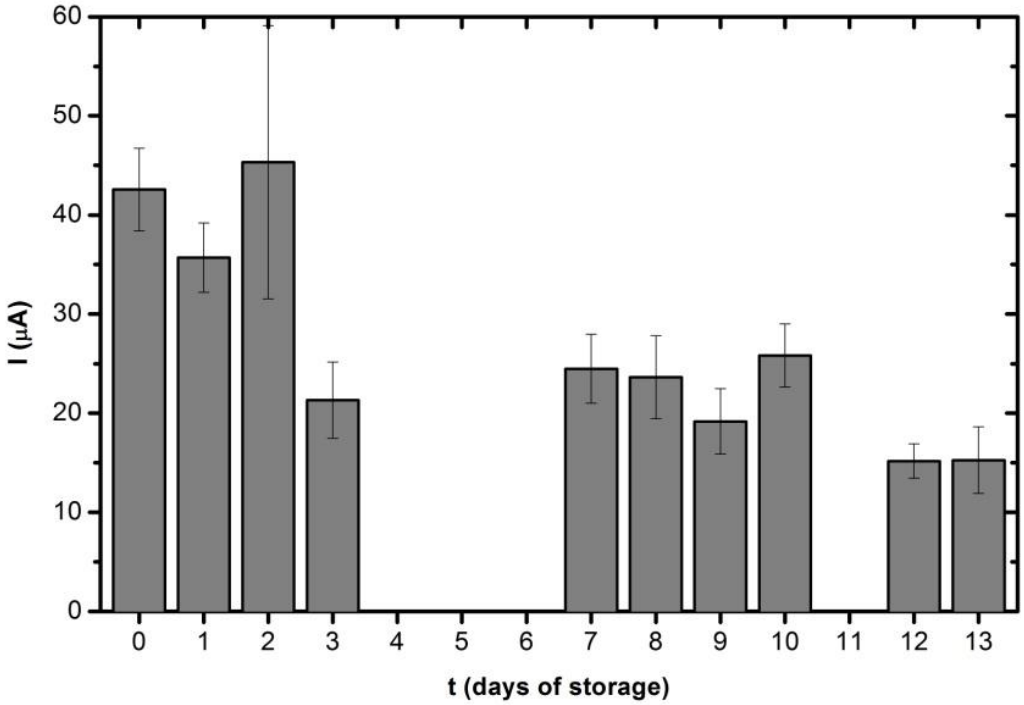

Figure S4. A storage stability of the TP|KB-PLA-based biofuel cell. Current response for each day is taken as an average value of a 3 h continuous measurement of the BFC response biased at 300 mV. Measurement was done in an aerated 0.1 M acetate buffer containing 0.2 M fructose at pH 6.0.

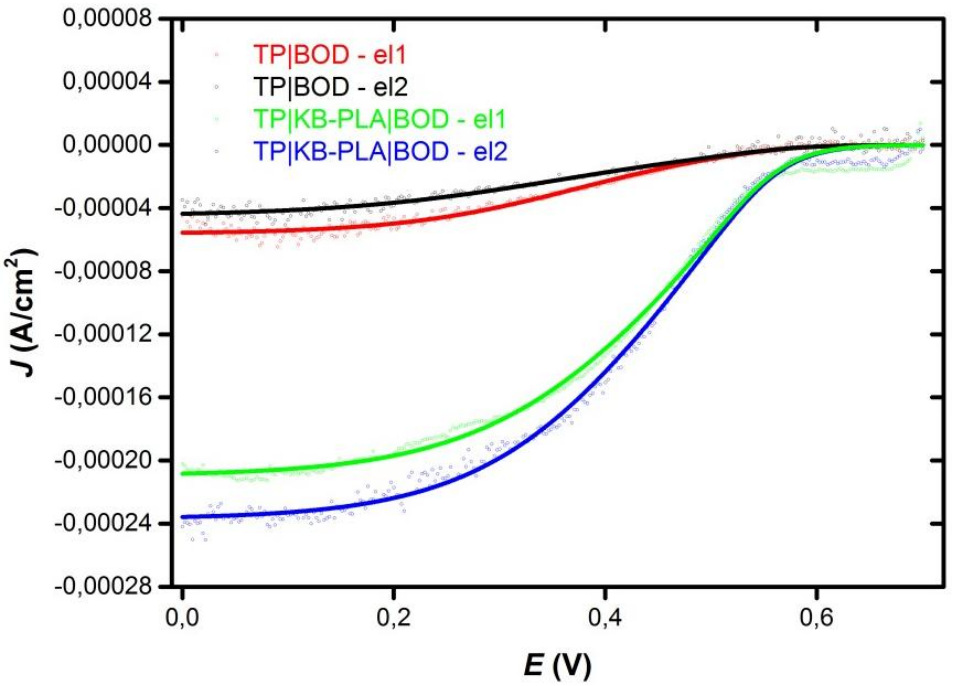

Figure S5. Reduction of oxygen on the biocathodes TP|KB-PLA|BOD and TP|BOD together with nonlinear fits of bioelectrocatalytic waves obtained under the conditions given in the text and evaluated using the aforementioned equations (1) – (3). Measurement was done in 0.1 M aerated acetate buffer pH 6.0 at a scan rate of 50 mV s^{-1}.

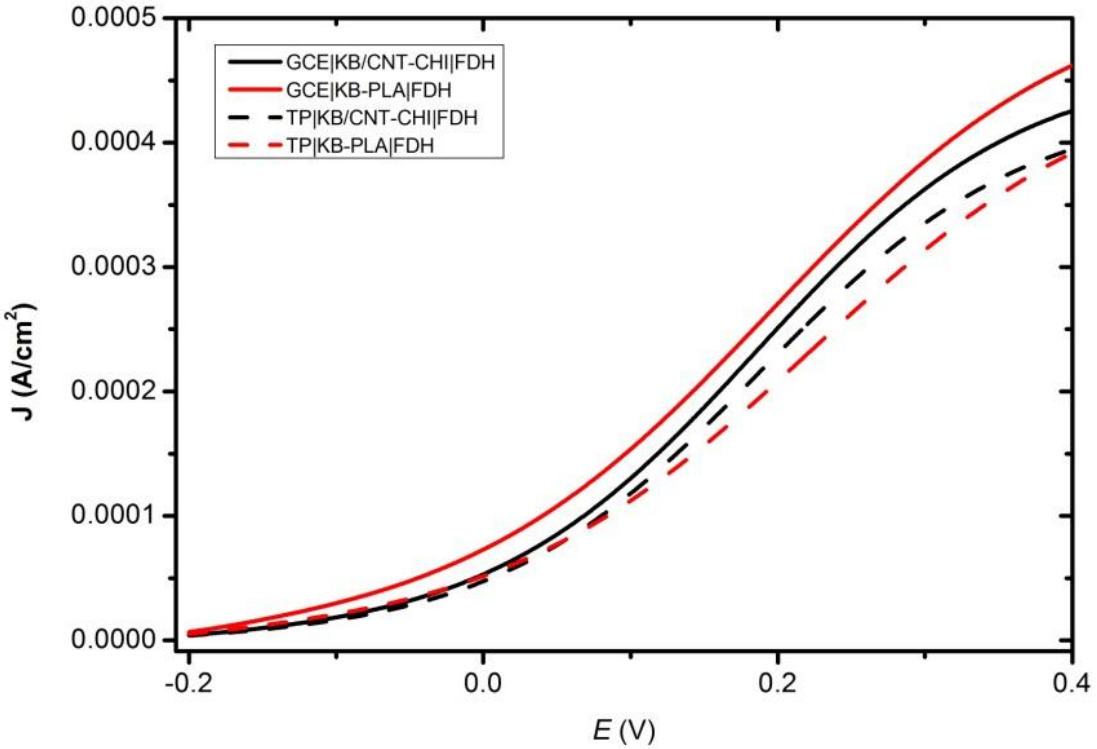

Figure S6. Nonlinear fits of measured anodic parts of background corrected CVs of GCE (solid lines) and TP (dashed lines) bioanodes based on chitosan (black curves) and PLA (red curves) composites. Fitted CVs were obtained under the conditions given in the text and evaluated using the aforementioned equations (1) – (3).

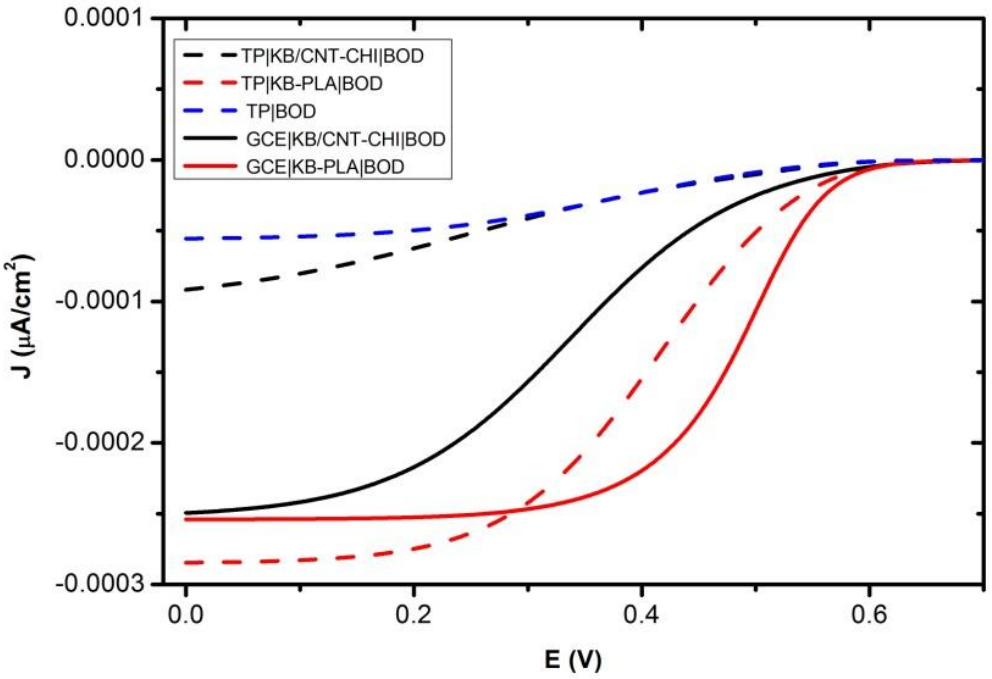

Figure S7. Nonlinear fits of measured cathodic parts of background corrected CVs of the biocathodes prepared on GCE (solid lines) and TP (dashed lines) from a chitosan (black curves) and PLA (red curves) nanocomposites. Moreover a nonlinear fit for the bioelectrocatalytic reduction of oxygen on the TP|BOD biocathode is shown, as well (blue dashed curve). Fitted CVs were obtained under the conditions given in the text and evaluated using the aforementioned equations (1) – (3).

Supplementary references

s1. T. Ikeda, D. Kobayashi, F. Matsushita, T. Sagara, K. Niki, *J. Electroanal. Chem.* 361 (1993) 221.
s2. S. Tsujimura, T. Nakagawa, K. Kano, T. Ikeda, *Electrochemistry* 72 (2004) 437.
s3. J. Marcinkeviciene, G. Johansson, *FEBS Letters* 318 (1993) 23.